Journal of Quantitative Spectroscopy & Radiative Transfer 144 (2014) 1–10

Contents lists available at ScienceDirect

Journal of Quantitative Spectroscopy & Radiative Transfer

journal homepage: www.elsevier.com/locate/jqsrt

High resolution analysis of the (111) vibrational state of SO_2

O.N. Ulenikov [a,b,*], O.V. Gromova [a,b], E.S. Bekhtereva [a,b], A.S. Belova [b], S. Bauerecker [c], C. Maul [c], C. Sydow [c], V.-M. Horneman [d]

[a] Institute of Physics and Technology, National Research Tomsk Polytechnic University, Tomsk 634050, Russia
[b] Physics Department, National Research Tomsk State University, Tomsk 634050, Russia
[c] Institut für Physikalische und Theoretische Chemie, Technische Universität Braunschweig, D-38106 Braunschweig, Germany
[d] Department of Physics, University of Oulu, P. O. Box 3000, FIN-90014, Finland

ARTICLE INFO

Article history:
Received 24 December 2013
Received in revised form
20 March 2014
Accepted 24 March 2014
Available online 30 March 2014

Keywords:
Sulfur dioxide
High-resolution spectra
Spectroscopic parameters
Hot band

ABSTRACT

The high resolution Fourier transform spectrum of the weak $\nu_1+\nu_2+\nu_3$ band was recorded and analyzed for the first time. 1085 transitions with values of quantum numbers $J^{max.}=65$ and $K_a^{max.}=21$ were assigned to that band. The hot band $\nu_1+\nu_2+\nu_3-\nu_2$ was also recorded and analyzed, and 1132 transitions with values of quantum numbers $J^{max.}=77$ and $K_a^{max.}=20$ were assigned. On the basis of the obtained information, 780 ro-vibrational energies of the (111) upper vibrational state were determined. The derived results significantly exceed analogous results known in the literature both in number of the assigned transitions and upper energy levels, and in values of quantum numbers $J^{max.}$ and $K_a^{max.}$.

1. Introduction

Sulfur dioxide is an important chemical species in many fields of both pure scientific and applied problems. It is a very important molecule because of its presence in Earth's polluted atmosphere. Sulfur dioxide is one of the air pollutants released in the atmosphere as a result of volcanic eruptions and of fuel combustion in human activities; it is one of the primary polluters of acid rain. To solve the problems of propagation of monochromatic radiation in the atmosphere, laser sounding, information transfer, the remote detection and monitoring of SO_2 in situ, etc., a good knowledge of the fine structure of the SO_2 absorption spectra in different parts of the electromagnetic spectrum is needed. As a consequence, over the years numerous laboratory spectroscopic studies of SO_2 have been reported in the literature (a comprehensive literature overview on the topic was presented in our recent paper [1]).

In the present work we continue our recent studies of the high resolution spectra of SO_2, Refs. [1–6]. We concentrate on the rotational structure of the (111) vibrational state, which was discussed earlier only in the context of high resolution analysis of the hot band $\nu_1+\nu_2+\nu_3-\nu_2$, Refs. [7–9] (no line-by-line analysis of the $\nu_1+\nu_2+\nu_3$ band has been reported before). In our present analysis, we were able to assign transitions of the $\nu_1+\nu_2+\nu_3-\nu_2$ hot band with values of quantum numbers J and K_a considerably higher than in Refs. [7–9]. Moreover, transitions of the weak $\nu_1+\nu_2+\nu_3$ cold band also were recorded and assigned for the first time. Section 2 describes the experimental conditions for the recorded spectra. In Section 3 we briefly present the Hamiltonian model used to fit the experimental line positions. Description of the spectra, assignment of transitions, and the results of analysis of the

* Corresponding author at: Institute of Physics and Technology, National Research Tomsk Polytechnic University, Tomsk 634050, Russia. Tel.: +7 962 785 9656.
E-mail address: ulenikov@mail.ru (O.N. Ulenikov).

http://dx.doi.org/10.1016/j.jqsrt.2014.03.027
0022-4073/

high resolution spectra of the bands $\nu_1+\nu_2+\nu_3$ and $\nu_1+\nu_2+\nu_3-\nu_2$ as well as the determination of spectroscopic parameters of the state (111) are presented in Section 4.

2. Experimental details

The experimental spectra in the region of 2950–3050 cm^{-1} and 2400–2550 cm^{-1} were recorded with Bruker IFS-120HR Fourier transform spectrometers in the Infrared Laboratory of University of Oulu and in Technische Universität, Braunschweig, respectively. The SO_2 sample, made by Sigma-Aldrich Inc., with purity of 99.9% was studied with an absorption spectroscopic method in multipath White cells in Oulu, [10], and Braunschweig.

For the region of 2950–3050 cm^{-1}, the sample pressure was 111 Pa and the absorption path length was 163.2 m. The cell was provided with two 6 mm thick potassium bromide windows. A Globar source, KBr beamsplitter and an indium antimonide semiconductor detector were used. The final spectral resolution limited mainly by Doppler broadening is about 0.0054 cm^{-1} around the band center. The measurements of these weak spectra required rather long recording times. In this case the registration time was 80.5 h. The spectrum was calibrated with 326 OCS lines [11]. The peak positions were calculated with the optimized center of gravity method discussed in Ref. [12].

Two spectra have been recorded for the region of 2400–2550 cm^{-1} to analyze the $\nu_1+\nu_2+\nu_3-\nu_2$ hot band which is covered by the stronger $\nu_1+\nu_3$ band. In each case the sample pressure was 150 Pa and a tungsten light source, a CaF_2 beamsplitter as well as an indium antimonide detector were used. In the one, the absorption pathlength was 4 m and 650 scans (18.4 h) have been recorded resulting in a nearly saturated spectrum, in the other case 24 m and 460 scans (13.0 h) have been chosen resulting in an oversaturated spectrum. As in the Oulu results described above, also in the Braunschweig measurements the final spectral resolution was mainly limited by Doppler broadening and resulted in 0.0048 cm^{-1} while an instrumental resolution of 0.0035 cm^{-1} was used for both spectra. Furthermore the $\nu_1+\nu_2+\nu_3$ band in the 2900–3100 cm^{-1} region has also been measured in Braunschweig (300 Pa, 48 m, 1260 scans) with slightly lower signal-to-noise quality and supports the Oulu result. The wavenumber accuracy of non-blended, unsaturated and not too weak lines can be estimated to be better than 10^{-4} cm^{-1} in both the ranges. Experimental conditions for all recorded spectra are summarized in Table 1.

3. Hamiltonian model

The SO_2 molecule is an asymmetric top with the value of asymmetry parameter, $\kappa=(2B-A-C)/(A-C)\approx -0.94$, being close to the prolate symmetric top limit. Because of the C_{2v} symmetry, three vibrational modes of SO_2 possess the following symmetry: $q_\lambda \in A_1$ for $\lambda=1, 2$, and $q_\lambda \in B_1$ for $\lambda=3$. As a consequence, two types of bands are allowed in absorption: A_1-type bands that correspond to the vibrational transitions $(v_{A_1})\leftarrow(v_{gr.})$, and B_1-type bands that correspond to the vibrational transitions $(v_{B_1})\leftarrow(v_{gr.})$.

Table 1
Experimental setup for the regions 2900–3100 cm^{-1} and 2400–2550 cm^{-1} of the infrared spectrum of SO_2.

Region (cm^{-1})	Institute	Resolution (cm^{-1})	Measuring time (h)	Source	Detector	Beam-splitter	Opt. path-length (mm)	Aperture (mm)	Temp. (°C)	Pressure (Pa)	Calibr.gas
2400–2550	Braunschw.	0.0048	18.4	Tungsten	InSb	CaF_2	4.0	1.15	23 ± 0.5	150 ± 2	CO_2, CO
2400–2550	Braunschw.	0.0048	13.0	Tungsten	InSb	CaF_2	24.0	1.15	23 ± 0.5	150 ± 2	CO_2, CO
2950–3050	Oulu	0.0054	80.5	Globar	InSb	KBr	163.2		Roomt.	111	OCS
2900–3100	Braunschw.	0.0036	36.1	Tungsten	InSb	CaF_2	48 ± 1	1.15	23 ± 0.5	300 ± 3	H_2O

As discussed earlier (see, *e.g.*, Refs. [13–16]), the presence of local resonance interactions is distinct to the high resolution spectra of SO_2. As a consequence, a Hamiltonian which takes into account the presence of resonance interactions, both Fermi and Coriolis types, should be used for analysis of high resolution spectra of the SO_2 molecule. Such effective Hamiltonian, applied for asymmetric top molecules, has been discussed in the spectroscopic literature (see, *e.g.*, Refs. [17,18]). For the XY_2-type molecule of the C_{2v} symmetry an effective Hamiltonian of a set of interacting states has the following form:

$$H^{v.-r.}=\sum_{v,\tilde{v}}|v\rangle\langle\tilde{v}|H_{v\tilde{v}}, \tag{1}$$

where the summation extends over all interacting vibrational states. The diagonal operators H_{vv} describe unperturbed rotational structures of the corresponding vibrational states. The nondiagonal operators $H_{v\tilde{v}}$, $(v\neq\tilde{v})$ describe resonance interactions (Fermi or Coriolis) between the states $|v\rangle$ and $|\tilde{v}\rangle$. The diagonal block operators have the same form for any vibrational state involved in the consideration (Watson's Hamiltonian in the *A*-reduction and I^r representation, Ref. [17]):

$$\begin{aligned}H_{vv}=&E^v+[A^v-\tfrac{1}{2}(B^v+C^v)]J_z^2+\tfrac{1}{2}(B^v+C^v)J^2+\tfrac{1}{2}(B^v-C^v)J_{xy}^2\\&-\Delta_K^vJ_z^4-\Delta_{JK}^vJ_z^2J^2-\Delta_J^vJ^4-\delta_K^v[J_z^2,J_{xy}^2]-2\delta_J^vJ^2J_{xy}^2\\&+H_K^vJ_z^6+H_{KJ}^vJ_z^4J^2+H_{JK}^vJ_z^2J^4+H_J^vJ^6+[J_{xy}^2,h_K^vJ_z^4+h_{JK}^vJ^2J_z^2+h_J^vJ^4]\\&+L_K^vJ_z^8+L_{KKJ}^vJ_z^6J^2+L_{JK}^vJ_z^4J^4+L_{KJJ}^vJ_z^2J^6+L_J^vJ^8\\&+[J_{xy}^2,l_K^vJ_z^6+l_{KJ}^vJ^2J_z^4+l_{JK}^vJ^4J_z^2+l_J^vJ^6]+\cdots,\\&+P_K^vJ_z^{10}+P_{KKKJ}^vJ_z^8J^2+P_{KKJ}^vJ_z^6J^4+P_{JJK}^vJ_z^4J^6\\&+S_K^vJ_z^{12}+S_{KKKKJ}^vJ_z^{10}J^2+\cdots\end{aligned} \tag{2}$$

where J_α $(\alpha=x, y, z)$ are the components of the angular momentum operator defined in the molecule-fixed coordinate system; $J_{xy}^2=J_x^2-J_y^2$; A^v, B^v, and C^v are the effective rotational constants connected with the vibrational states v, and the other parameters are the different order centrifugal distortion coefficients.

Because of the symmetry arguments of the SO_2 molecule, the nondiagonal block operators can only be of two types: Fermi interactions and Coriolis interactions of the B_1-symmetry. In this case, the Fermi interaction operator has the form

$$\begin{aligned}{}^FH_{v\tilde{v}}=&{}^{vv}F_0+{}^{vv}F_KJ_z^2+{}^{vv}F_JJ^2+\cdots+{}^{vv}F_{xy}(J_x^2-J_y^2)\\&+{}^{vv}F_{Kxy}\{J_z^2,(J_x^2-J_y^2)\}_+ +2{}^{vv}F_{Jxy}J^2(J_x^2-J_y^2)+\cdots\end{aligned} \tag{3}$$

The corresponding Coriolis interaction operator can be written as

$$\begin{aligned}{}^CH_{v\tilde{v}}=&iJ_yH_{v\tilde{v}}^{(1)}+H_{v\tilde{v}}^{(1)}iJ_y+\{J_x,J_z\}_+H_{v\tilde{v}}^{(2)}+H_{v\tilde{v}}^{(2)}\{J_x,J_z\}_+\\&+\{iJ_y,(J_x^2-J_y^2)\}_+H_{v\tilde{v}}^{(3)}+H_{v\tilde{v}}^{(3)}\{iJ_y,(J_x^2-J_y^2)\}_+ +\cdots,\end{aligned} \tag{4}$$

where the operators $H_{v\tilde{v}}^{(i)}$, $i=1, 2, 3$, in Eq. (4) are

$${}^CH_{v\tilde{v}}{}^{(i)}=\tfrac{1}{2}{}^{vv}C^i+{}^{vv}C_K^iJ_z^2+\tfrac{1}{2}{}^{vv}C_J^iJ^2+{}^{vv}C_{KK}^iJ_z^4+\cdots \tag{5}$$

4. Analysis of spectra and determination of spectroscopic parameters

In the present study we analyze the rotational structure of the (111) vibrational state. In this case, the transitions of the band $\nu_1+\nu_2+\nu_3$ (which was not analyzed before) and of the hot band $\nu_1+\nu_2+\nu_3-\nu_2$ (considerably larger number of assigned transitions with higher values of quantum numbers J and K_a than it was discussed in the spectroscopic literature) have been used for determination of upper ro-vibrational energies. In the upper part of Fig. 1 one can see a survey spectrum of the $\nu_1+\nu_2+\nu_3$ band. The spectrum is weak, but all three branches (both P-, Q-, and R-branches) are clearly pronounced. Fig. 2 presents a small fragment of the P-branch with a few marked lines of the $\nu_1+\nu_2+\nu_3-\nu_2$ band.

Both the $\nu_1+\nu_2+\nu_3$ and the $\nu_1+\nu_2+\nu_3-\nu_2$ bands are of B_1-type. As a consequence, the selection rules for "allowed" transitions in both bands are

$$\Delta J=0,\pm1,\quad \Delta K_a=0,\quad \Delta K_c=\pm1.$$

Besides "allowed" transitions, weak "forbidden" ones are allowed with more general selection rules:

$$\Delta J=0,\pm1,\quad \Delta K_a=even,\quad \Delta K_c=odd.$$

Assignments of transitions were made on the basis of the Combination Differences method. In this case, the rotational energies of the lower vibrational states were calculated with the improved parameters of the ground vibrational state, Ref. [1], and parameters of the (010) vibrational state from Ref. [19]. As a result, the 1085 transitions with the maximum values of quantum numbers $J^{max.}=65$ and $K_a^{max.}=21$ have been assigned to the $\nu_1+\nu_2+\nu_3$ band (see also statistical information in Table 1). Analogously, the 1132 transitions with the maximum values of quantum numbers $J^{max.}=77$ and $K_a^{max.}=20$ have been assigned to the $\nu_1+\nu_2+\nu_3-\nu_2$ band. It is important that the experimental data from the bands $\nu_1+\nu_2+\nu_3$ and $\nu_1+\nu_2+\nu_3-\nu_2$ mutually add each other. In this case, transitions with lower values of quantum numbers J and K_a could be poorly determined from the hot $\nu_1+\nu_2+\nu_3-\nu_2$ band, but have been obtained with a good accuracy from the $\nu_1+\nu_2+\nu_3$ band. On the other hand, transitions with higher values of quantum numbers J and K_a are absent in the $\nu_1+\nu_2+\nu_3$ band, but can be found in the wings of the P- and R-branches of the hot band $\nu_1+\nu_2+\nu_3-\nu_2$. The complete list of the assigned transitions is presented as Supplementary material S1 in this paper.

One remark should be made here. Because the spectra were recorded not only in the different spectral regions, but also with two different Fourier transform spectrometers (Oulu, Finland and Braunschweig, Germany), the line positions in the region 2400–2550 cm^{-1} have been post-calibrated in accordance with the positions of lines of the spectrum in the region 2950–3050 cm^{-1}. To realize that, we used 10 ro-vibrational energies of the state (111) which have been correctly determined from transitions of the $\nu_1+\nu_2+\nu_3$ band on the basis of the Ground State Combination Differences method. Then transitions to the same 10 upper ro-vibrational states were assigned in

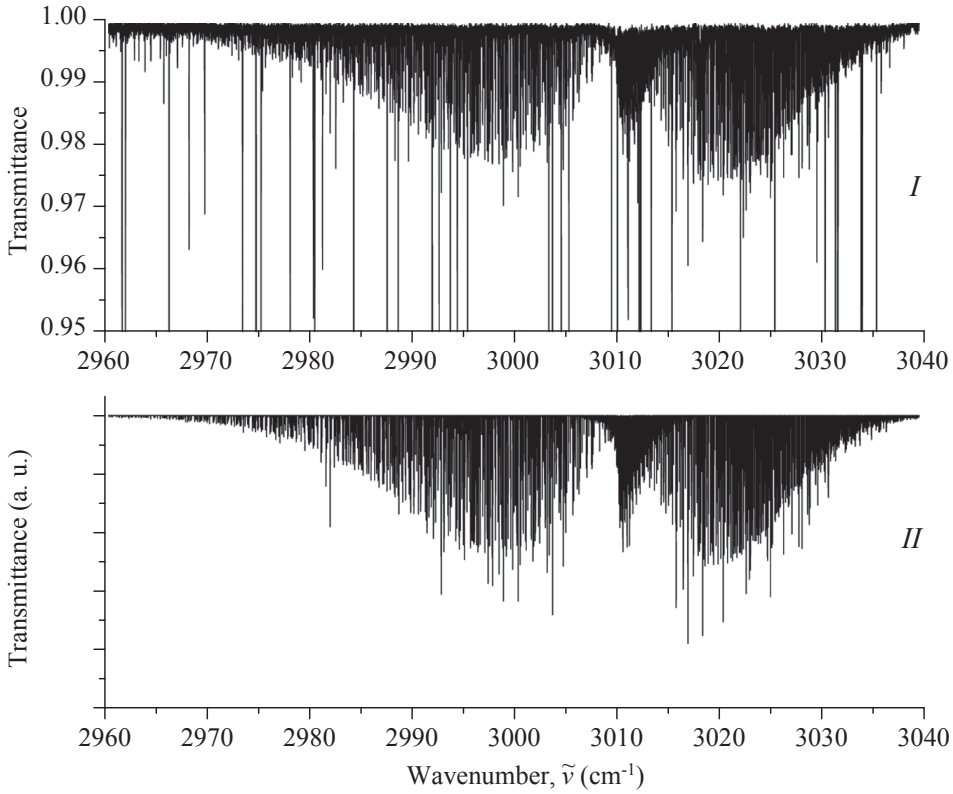

Fig. 1. Survey spectrum of SO_2 in the region of the weak $\nu_1+\nu_2+\nu_3$ band. Experimental conditions: absorption path length is 163.2 m; sample pressure is 111 Pa; room temperature; registration time is 80.5 h. The simulated spectrum is shown in the lower part of the figure.

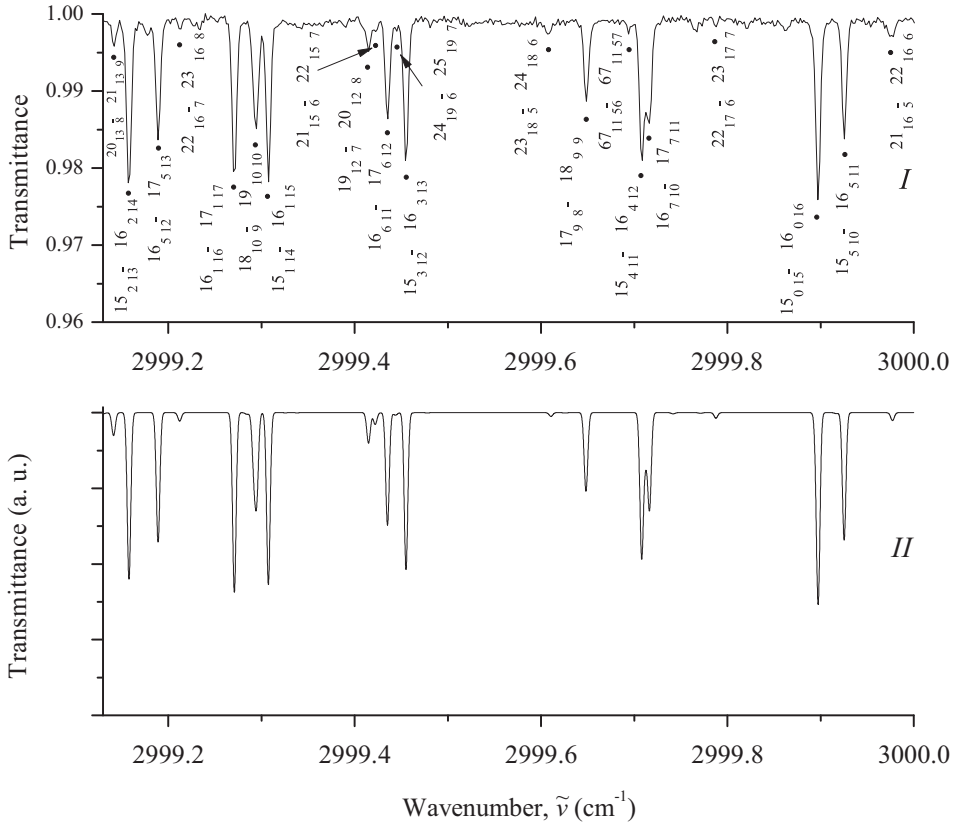

Fig. 2. Small portion of the high resolution spectrum of SO_2 in the region of the *P*-branch of the $\nu_1+\nu_2+\nu_3$ band (upper part). Experimental conditions: absorption path length is 163.2 m; sample pressure is 111 Pa; room temperature; registration time is 80.5 h. The simulated spectrum is shown in the lower part of the figure.

Table 2
Statistical information for the (111) vibrational state of SO_2.

Band 1	Center[a] 2	$E_{(111)}$[a] 3	J^{max} 4	K_a^{max} 5	N_t[b] 6	N_{el}[c] 7	rms[d] 8	m_1[e] 9	m_2[e] 10	m_3[e] 11
$\nu_1+\nu_2+\nu_3-\nu_2$ [7]	2492.444(8)		39	10	107					
$\nu_1+\nu_2+\nu_3-\nu_2$ [9]		3010.31730(20)	44	16		247	1.4	89.9	8.5	1.6
$\nu_1+\nu_2+\nu_3$, tw	3010.317420	3010.317401(14)	65	21	1085	780	1.26	90.8	8.2	1.0
$\nu_1+\nu_2+\nu_3-\nu_2$, tw	2492.444990	3010.317401(14)	77	20	1132	780	1.26	90.8	8.2	1.0

[a] In cm^{-1}.
[b] N_t is the number of assigned transitions.
[c] N_{el} is the number of obtained upper-state energy levels.
[d] In 10^{-4} cm^{-1}.
[e] Here $m_i = n_i/N_{el} \times 100\%$ (i = 1, 2, 3); n_1, n_2, and n_3 are the numbers of upper-state energies for which the differences $\delta = E^{exp} - E^{calc}$ satisfy the conditions $\delta \le 2 \times 10^{-4}$ cm^{-1}, 2×10^{-4} cm^{-1} $< \delta \le 4 \times 10^{-4}$ cm^{-1}, and $\delta > 4 \times 10^{-4}$ cm^{-1}.

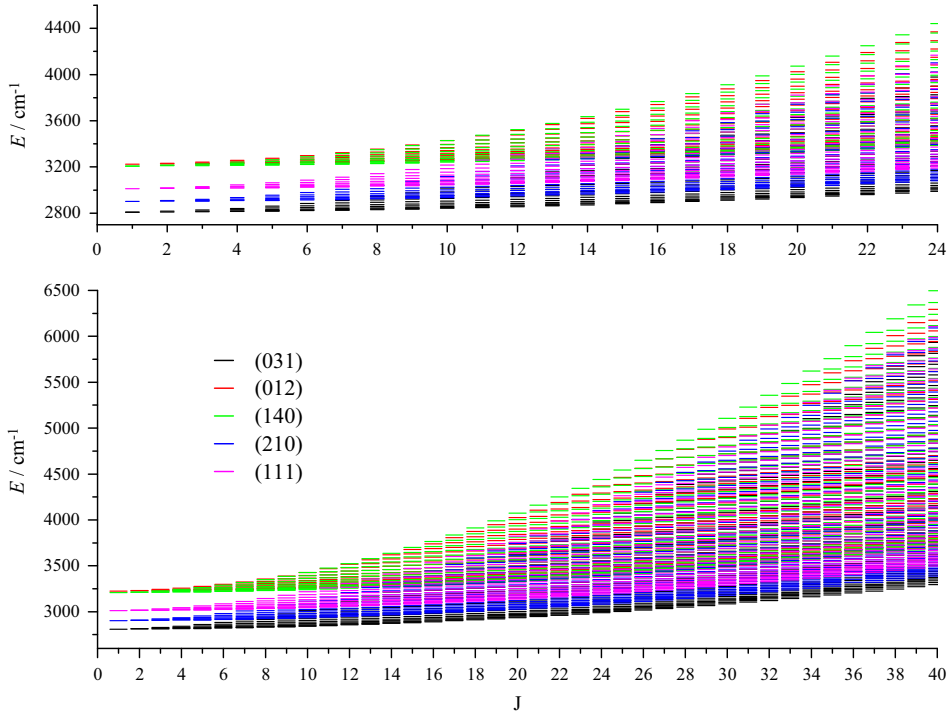

Fig. 3. Diagram of ro-vibrational energy levels of the (111), (210), (012), (140), and (031) vibrational states of SO_2 as functions of the rotational quantum number J. Different colors indicate ro-vibrational energy levels belonging to different vibrational states. (For interpretation of the references to color in this figure caption, the reader is referred to the web version of this paper.)

the $\nu_1+\nu_2+\nu_3-\nu_2$ hot band. As the analysis shows, the mean difference between expected and experimental line positions of the hot band $\nu_1+\nu_2+\nu_3-\nu_2$, which were involved in such analysis, was 0.00231 cm^{-1}. Finally, all the experimental line positions in the region of 2400–2550 cm^{-1} were calibrated in accordance with the obtained value of 0.00231 cm^{-1}.

Transitions assigned to both the $\nu_1+\nu_2+\nu_3$ and $\nu_1+\nu_2+\nu_3-\nu_2$ bands were then used for determination of the upper ro-vibrational energies, which are presented in column 2 of Supplementary material S2 in this paper (for illustration, a small fragment of S2 is shown in Table 3; see also the statistical information in Table 2). In many cases, for high values of the quantum number J the upper energies were defined from single transitions. It follows from the fact that, even in the wings of the band, lines of the hot band are covered very often by the lines of the considerably stronger $\nu_1+\nu_3$ band. Finally, the 780 obtained upper energies with maximum values of quantum numbers $J^{max.} = 77$ and $K_a^{max.} = 21$ were used as an initial data in the fit of parameters of the effective Hamiltonian, Eqs. (1)–(5).

Following the strategy of Ref. [1], we took into account interactions between the studied vibrational state (111), on the one hand, and vibrational states (210) and (012) (Coriolis interactions) and (031) (Fermi interaction), on the other hand (Fig. 3 gives an impression of the ro-vibrational energy structure in the studied region). The values of spectroscopic parameters for the states (210) and (012) have been taken from Ref. [6] and were fixed in the fit procedure. In this case, because of strong local resonance interactions between the states (012) and (140)

Table 3
Small Part of Experimental Ro-vibrational Term Values for the (111) Vibrational State of the SO_2 Molecule (in cm^{-1}).[a]

J	K_a	K_c	E	N	Δ	δ	J	K_a	K_c	E	N	Δ	δ	J	K_a	K_c	E	N	Δ	δ
1			2	3	4	5	1			2	3	4	5	1			2	3	4	5
17	8	9	3217.50387	4	7	3	19	18	1	3681.93769	1		−7	22	3	20	3186.21772	3	9	1
17	9	8	3246.69322	5	23	10	19	19	0	3743.76393	1		18	22	4	19	3198.56215	4	6	3
17	10	7	3279.25927	5	34	−7	20	1	20	3137.96950	4	15	3	22	5	18	3213.91969	2	12	−2
17	11	6	3315.18063	4	8	−3	20	2	19	3148.63754	3	7	7	22	6	17	3232.75943	4	10	1
17	12	5	3354.43406	1		5	20	3	18	3159.00075	4	2	5	22	7	16	3255.08243	4	24	8
17	13	4	3396.99499	2	19	4	20	4	17	3171.20022	4	16	−11	22	8	15	3280.84803	5	8	7
17	15	2	3491.93466	3	17	−9	20	5	16	3186.59697	4	5	3	22	9	14	3310.02535	4	18	−2
17	16	1	3544.25778	2	4	5	20	6	15	3205.47870	5	14	−4	22	10	13	3342.58876	3	4	7
17	17	0	3599.77675	3	12	9	20	7	14	3227.82600	4	14	−4	22	12	11	3417.77489	4	7	4
18	1	18	3114.74283	3	22	1	20	8	13	3253.60495	3	5	2	22	13	10	3460.34767	3	9	6
18	2	17	3124.42890	3	8	−5	20	9	12	3282.78897	5	14	−3	22	14	9	3506.20516	3	8	1
18	3	16	3134.28473	4	6	−4	20	10	11	3315.35455	4	12	−11	22	15	8	3555.31981	2	10	6
18	4	15	3146.40063	2	4	6	20	11	10	3351.27880	4	11	8	22	16	7	3607.66252	2	17	5
18	5	14	3161.83640	3	6	−4	20	12	9	3390.53727	3	15	−2	22	17	6	3663.20304	5	25	−13
18	6	13	3180.75011	5	7	7	20	13	8	3433.10541	3	17	−4	22	18	5	3721.91056	1		−2
18	7	12	3203.11481	4	5	2	20	14	7	3478.95705	4	13	7	22	21	2	3916.70518	1		15
18	8	11	3228.90265	4	10	−8	20	15	6	3528.06444	1		7	23	0	23	3177.14234	4	5	4
18	9	10	3258.09081	3	12	0	20	16	5	3580.39882	5	30	−3	23	1	22	3188.70711	3	8	6
18	11	8	3326.57957	4	17	−2	20	17	4	3635.93034	2	41	−5	23	2	21	3196.59168	3	9	−4
18	12	7	3365.83490	2	12	13	20	20	1	3821.39058	1		26	23	3	20	3203.23708	3	5	2
18	13	6	3408.39814	1		2	21	0	21	3150.39650	3	7	−2	23	4	19	3213.54930	4	13	−3
18	14	5	3454.24383	2	5	13	21	1	20	3160.58427	3	12	−4	23	5	18	3228.56631	4	8	3
18	15	4	3503.34408	4	33	−7	21	2	19	3167.30339	4	14	13	23	6	17	3247.35909	4	9	3
18	16	3	3555.67117	1		33	21	3	18	3173.90920	5	10	−4	23	7	16	3269.66586	4	12	−1
19	0	19	3125.96284	4	9	−1	21	4	17	3184.73687	5	14	9	23	8	15	3295.42294	4	19	1
19	1	18	3134.75551	4	9	−3	21	5	16	3199.94703	3	6	−1	23	9	14	3324.59583	4	12	−1
19	2	17	3140.53157	4	6	−4	21	6	15	3218.80012	4	7	1	23	10	13	3357.15727	3	19	5
19	3	16	3147.30115	3	4	8	21	8	13	3266.90864	6	22	−7	23	11	12	3393.08177	4	17	−1
19	4	15	3158.56211	3	8	−5	21	9	12	3296.08991	3	9	8	23	12	11	3432.34426	3	12	−12
19	5	14	3173.90024	5	3	0	21	10	11	3328.65447	6	17	−8	23	13	10	3474.91935	3	33	4
19	6	13	3192.79583	5	11	7	21	11	10	3364.57910	4	11	2	23	14	9	3520.77996	3	22	12
19	7	12	3215.15239	3	12	−8	21	12	9	3403.83908	3	10	−9	23	15	8	3569.89807	3	17	−4
19	8	11	3240.93635	4	6	0	21	13	8	3446.40938	3	17	−28	23	16	7	3622.24495	3	16	−13
19	9	10	3270.12281	4	13	9	21	14	7	3492.26416	5	12	−3	23	17	6	3677.79061	2	22	6
19	10	9	3302.68882	2	12	−9	21	15	6	3541.37533	2	31	16	23	18	5	3736.50330	2	19	12
19	11	8	3338.61223	5	17	−2	21	16	5	3593.71396	3	24	24	24	1	24	3191.41003	4	9	3
19	12	7	3377.86911	4	16	−6	21	17	4	3649.24988	2	8	10	24	2	23	3204.21526	3	21	−10
19	13	6	3420.43492	5	31	−2	21	18	3	3707.95230	2	21	18	24	3	22	3215.91611	2	6	−1
19	14	5	3466.28340	3	28	−7	21	20	1	3834.72510	1		−39	24	4	21	3228.48266	1		6
19	15	4	3515.38730	4	13	−6	21	21	0	3902.72873	2	11	−34	24	5	20	3243.81001	4	7	0
19	16	3	3567.71772	2	29	−16	22	1	22	3163.52656	4	8	7	24	6	19	3262.59655	4	13	−9
19	17	2	3623.24496	3	16	−10	22	2	21	3175.23882	2	3	5	24	7	18	3284.88676	3	15	−4

[a] In Table 3, N is the number of transitions which were used for determination of upper energy value; Δ is the experimental uncertainty in the upper energy value in units of 10^{-5} cm^{-1} (Δ is absent when the upper energy value was determined from a single transition); δ is the difference $E^{exp.}-E^{calc.}$ also in units of 10^{-5} cm^{-1}.

which were discussed in Ref. [6], the state (140) was also taken into account in our fit. Parameters of all three mentioned states, (210), (012), and (140), are shown in columns 5–7 of Table 4).

Parameters of the (031) vibrational state (with the exception of the vibrational energy E) have been estimated in accordance with the same scheme as was presented by Eqs. (9)–(11) of Ref. [6]:

$$P^{(031)} = P^{(030)} + P^{(001)} - P^{(000)}, \quad (6)$$

$$P^{(0v0)} = P^{(000)} + \alpha v + \beta v^2 \quad (7)$$

and, as a consequence,

$$P^{(030)} = P^{(000)} + 3(P^{(020)} - P^{(010)}). \quad (8)$$

Here $P^{(v_1v_2v_3)}$ is any of the rotational, A, B, C, or centrifugal distortion, Δ_K, Δ_{JK}, Δ_J, etc., parameters of the $(v_1v_2v_3)$ vibrational state; α and β coefficients can be determined from the values of parameters $P^{(000)}$, $P^{(010)}$, and $P^{(020)}$ of the vibrational states (000), (010), and (020) in accordance with the formula (7), respectively. In our case, the parameters $P^{(000)}$, $P^{(010)}$, and $P^{(020)}$ have been taken from Refs. [19] and [1], respectively. Parameters of the (031) vibrational state, obtained on the basis of Eqs. (6)–(8), are shown in column 8 of Table 4. The value of the vibrational energy, E, was estimated on the basis of parameters of the intramolecular potential function from Refs. [3,20].

The initial values of the parameters $P^{(111)}$ were estimated with the simple formula:

$$P^{(111)} = P^{(100)} + P^{(010)} + P^{(001)} - 2P^{(000)}, \quad (9)$$

Table 4
Spectroscopic parameters of the (111) and some other vibrational states of the SO_2 molecule (in cm^{-1}).[a]

Parameter	(010)[b]	(111)[c]	(111)[d]	(210)[e]	(012)[e]	(140)[e]	(031)[f]
1	2	3	4	5	6	7	8
E	517.872430	3010.4367	3010.2307087(144)	2807.1880897	3222.9725043	3206.6520	2900.8888
A	2.0665903306	2.0469523609	2.046275617(448)	2.069176667	2.024244956	2.196	2.12987684
B	0.34425139494	0.34141448197	0.341395316(184)	0.3409396413	0.3419057161	0.3428	0.343203589
C	0.29299790750	0.29048837307	0.290419077(176)	0.2902074164	0.2907799020	0.290	0.290689990
$\Delta_K \times 10^4$	0.95810872	0.95663242	0.9542855(258)	0.9864890	0.92709739	1.323	1.16368204
$\Delta_{JK} \times 10^5$	−0.40713108	−0.40952552	−0.3889988(453)	−0.3776287	−0.4409517	−0.4541	−0.44723746
$\Delta_J \times 10^6$	0.2210206	0.2227101	0.2249916(312)	0.21953662	0.22603974	0.2201	0.2252111
$\delta_K \times 10^5$	0.1035275	0.1043185	0.1157770(428)	0.1213483	0.0921	0.175	0.14639669
$\delta_J \times 10^7$	0.57074622	0.57548431	0.577122(130)	0.5667696	0.5846	0.5796	0.58314824
$H_K \times 10^7$	0.153334	0.153685	0.1544340(398)	0.1634410	0.1468	0.2829	0.2090504
$H_{KJ} \times 10^9$	−0.7569297	−0.7660090	−0.91818(132)	−0.95079	−0.6752	−1.129	−0.9742572
$H_{JK} \times 10^{11}$	0.45728	0.45728	0.45728	0.45728	2.122	0.03066	1.1393911
$H_J \times 10^{12}$	0.374579	0.379477	0.34095(201)	0.374579	0.3775	−0.2925	0.379117
$h_K \times 10^9$	0.761006	0.770308	0.94491(523)	0.761006	1.438	1.162	1.15916
$h_{JK} \times 10^{11}$	−0.077103	−0.077103	−0.077103	−0.077103	−0.1064	−1.136	−0.185904
$h_J \times 10^{12}$	0.183225	0.186612	0.18614(182)	0.183225	0.1985	0.2426	0.185723
$L_K \times 10^{11}$	−0.372154	−0.371130	−0.371130	−0.372154	−0.3797	−0.4563	−0.569518
$L_{KKJ} \times 10^{12}$	0.23830	0.23860	0.23860	0.23830	0.2110	−0.4729	0.349807
$L_{JK} \times 10^{13}$	−0.1543	−0.1550	−0.1550	−0.1543	0.07973	0.07973	−0.2447261
$L_{JJK} \times 10^{16}$	−0.404	−0.404	−0.404	−0.404	−4.010	−4.010	−1.044808
$L_J \times 10^{17}$	−0.1060	−0.0973	−0.0973	−0.1060	−0.4554	−0.4554	−0.07076
$l_K \times 10^{12}$	−0.4530	−0.4547	−0.4547	−0.4530			−0.724644
$l_{KJ} \times 10^{14}$	0.274	0.304	0.304	0.274			0.251416
$l_{JK} \times 10^{17}$	−0.24	−0.24	−0.24	−0.24			
$l_J \times 10^{18}$	−0.64438	−0.64438	−0.64438	−0.64438			−0.749978
$P_K \times 10^{14}$	0.1046	0.1031	0.1031	0.1046	0.1167	0.1167	0.174486
$P_{KKKJ} \times 10^{16}$	−0.58867	−0.58867	−0.58867	−0.58867	−0.3237	−0.3237	−0.993503
$P_{KKJ} \times 10^{18}$	−0.9947	−0.9947	−0.9947	−0.9947			−1.497663
$P_{JJK} \times 10^{18}$	0.1222	0.1222	0.1222	0.1222			0.1981369
$S_K \times 10^{18}$	−0.226	−0.226	−0.226	−0.226			−0.400587
$S_{KKKKJ} \times 10^{19}$	0.1156	0.1156	0.1156	0.1156			0.219236
${}^{(111)/(031)}F_0$		3.08	3.08				
${}^{(111)/(031)}F_J$			$0.46308(298) \times 10^{-3}$				
${}^{(111)/(031)}F_{xy}$		0.123676×10^{-6}	0.123676×10^{-6}				
${}^{(210)/(111)}C^{(1)} = -{}^{(012)/(111)}C^{(1)}$		−0.24	−0.24				
${}^{(210)/(111)}C_K^{(1)} = -{}^{(012)/(111)}C_K^{(1)}$		-0.23829×10^{-4}	-0.23829×10^{-4}				

Table 4 (*continued*)

Parameter	(010)[b]	(111)[c]	(111)[d]	(210)[e]	(012)[e]	(140)[e]	(031)[f]
1	2	3	4	5	6	7	8
$^{(210)/(111)}C^{(2)} = -^{(012)/(111)}C^{(2)}$		0.29454 × 10^{-2}	0.29454 × 10^{-2}				
$^{(210)/(111)}C^{(3)} = -^{(012)/(011)}C^{(3)}$		0.44934 × 10^{-6}	0.44934 × 10^{-6}				
$^{(210)/(111)}C_J^{(3)} = -^{(012)/(111)}C_J^{(3)}$		−0.3302 × 10^{-11}	−0.3302 × 10^{-11}				
$^{(012)/(140)}F_0$		0.046234	0.046234				

[a] Values in parentheses are 1σ confidence intervals (in last digits). Parameters presented without confidence intervals were constrained to the predicted values (see text, for details).
[b] Reproduced from Ref. [19].
[c] Theoretically predicted (see text for details).
[d] Obtained from the fit.
[e] Reproduced from Ref. [6].
[f] Theoretically predicted (see text for details).

and $P^{(100)}$, $P^{(001)}$, $P^{(000)}$, and $P^{(010)}$ have been taken again from Refs. [1,19] (they are presented in column 3 of Table 4).

As to the resonance interaction parameters, they have been estimated in accordance with the relations:

$$^{(111)/(031)}F_{\dots} = \sqrt{3} \times {}^{(100)/(020)}F_{\dots} \tag{10}$$

for the Fermi-type interaction, and

$$^{(210)/(111)}C_{\dots} = -{}^{(012)/(111)}C_{\dots} = \sqrt{2} \times {}^{(100)/(001)}C_{\dots} \tag{11}$$

for the Coriolis-type interactions. The initial values of the parameters $^{(100)/(020)}F_{\dots}$ and $^{(100)/(001)}C_{\dots}$ were taken from Ref. [1], and the obtained values are shown at the bottom part of Table 4.

Values of spectroscopic parameters of the (111) vibrational state obtained from the fit are shown in column 4 of Table 4 together with 1σ statistical confidence intervals. Parameters presented in Table 4 without confidence intervals were constrained to their estimated values and were not changed in the fit procedure. Finally, a set of 15 fitted parameters reproduces the 780 initial energy values of the (111) vibrational state with the $d_{rms} = 1.26 \times 10^{-4}$ cm^{-1}, that can be considered as a good confirmation of correctness of the model used. Also for illustration of the correctness of the results, column 5 of Supplementary Material S2 and Table 3 present values of differences $\delta = E^{exp.} - E^{calc.}$ in units 10^{-5} cm^{-1}. From comparison of the values of fitted parameters of the (111) vibrational state with corresponding theoretically predicted values (columns 3 and 4 of Table 4), one can see good agreement between them, and with the parameters of the (010) state (see column 2). Also, as an illustration of the quality of the results obtained, the bottom parts of Figs. 1 and 2 present the simulated overview spectrum of the $\nu_1+\nu_2+\nu_3$ band and a small fragment of the *P*-branch. One can see very good agreements between experimental and simulated spectra.

It would be interesting to estimate how well the spectroscopic parameters known in the literature reproduce our set of experimental ro-vibrational energies. To answer that question, we made calculations of values of energy levels from Supplementary material S2 and Table 3 with the sets of parameters from Refs. [7,9] (they are reproduced in columns 4 and 5 of Table 5) and obtained d_{rms} values for both cases. They are 185.8×10^{-4} cm^{-1} and 4.8×10^{-4} cm^{-1} for the sets of parameters from [7,9], respectively. One can see that the first d_{rms} value is considerably worse in comparison with our $d_{rms} = 1.26 \times 10^{-4}$ cm^{-1}. The second d_{rms} value (it corresponds to the set of parameters from [9]) is only about three times worse than our d_{rms} value. At the same time, as followed from the vibration–rotation theory [21–24], the physically suitable values of parameters of the (111) vibrational state should be very close to the values of corresponding parameters of the (010) state (for convenience of the reader, the parameters of the (010) state from Ref. [19] are reproduced in column 2 of Table 5). However, as one can see from comparison of the data from columns 2 and 5, the values of high order parameters of Ref. [9] differ strongly from the values of corresponding parameters of the (010) state (see column 2). As to parameters obtained in the present study (see column 3

Table 5
Spectroscopic parameters of the (111) vibrational state (in cm^{-1}).

Parameter 1	(010) [19] 2	(111) tw 3	(111) [7] 4	(111) [9] 5
E	517.872430	3010.2307087	3010.317	3010.31730
A	2.0665903306	2.046275617	2.04635779	2.046364771
B	0.34425139494	0.341395316	0.34142571	0.341427396
C	0.29299790750	0.290419077	0.2904559	0.2904587583
$\Delta_K \times 10^4$	0.95810872	0.9542855	0.955825	0.95691534
$\Delta_{JK} \times 10^5$	−0.40713108	−0.3889988	−0.4086	−0.41624289
$\Delta_J \times 10^6$	0.2210206	0.2249916	0.2242	0.22274702
$\delta_K \times 10^5$	0.1035275	0.1157770	0.10721	0.1051414
$\delta_J \times 10^7$	0.57074622	0.577122	0.5786	0.5770256
$H_K \times 10^7$	0.153334	0.1544340	0.152296	0.1545055
$H_{KJ} \times 10^9$	−0.7569297	−0.91818	−0.7401	−0.754482
$H_{JK} \times 10^{11}$	0.45728	0.45728		0.15483
$H_J \times 10^{12}$	0.374579	0.34095	0.31488	0.32335
$h_K \times 10^9$	0.761006	0.94491	0.63754	0.742106
$h_{JK} \times 10^{11}$	−0.077103	−0.077103		−0.15789
$h_J \times 10^{12}$	0.183225	0.18614	0.167	0.186912
$L_K \times 10^{11}$	−0.372154	−0.371130		−0.35753
$L_{KKJ} \times 10^{12}$	0.23830	0.23860		0.1515
$L_{JK} \times 10^{13}$	−0.1543	−0.1550		0.0023664
$L_{JJK} \times 10^{16}$	−0.404	−0.404		1.518
$L_J \times 10^{17}$	−0.1060	−0.0973		0.5399
$l_K \times 10^{12}$	−0.4530	−0.4547		
$l_{KJ} \times 10^{14}$	0.274	0.304		
$l_{JK} \times 10^{17}$	−0.24	−0.24		
$l_J \times 10^{18}$	−0.64438	−0.64438		
$P_K \times 10^{14}$	0.1046	0.1031		0.06517
$P_{KKKJ} \times 10^{16}$	−0.58867	−0.58867		0.2589
$P_{KKJ} \times 10^{18}$	−0.9947	−0.9947		
$P_{JJK} \times 10^{18}$	0.1222	0.1222		
$S_K \times 10^{18}$	−0.226	−0.226		
$S_{KKKKJ} \times 10^{19}$	0.1156	0.1156		
$d_{rms} \times 10^4$		1.26	185.8	4.8

of Table 5), one can see good agreement between their values and values of corresponding parameters of column 2.

5. Conclusion

We analyzed for the first time the high resolution Fourier transform spectrum of the weak $\nu_1+\nu_2+\nu_3$ band of SO_2. The spectrum was recorded with the Bruker IFS-120HR Fourier transform spectrometer with a resolution of 0.0054 cm^{-1}. Additionally, Fourier transform spectra of the hot band $\nu_1+\nu_2+\nu_3-\nu_2$ were recorded with different sample pressures and optical pathlengths with the goal to assign transitions corresponding to high values of quantum numbers J and K_a. In general, 1085 and 1132 transitions with $J^{max.}/K_a^{max.} = 65/21$ and 77/20 were assigned to the bands $\nu_1+\nu_2+\nu_3$ and $\nu_1+\nu_2+\nu_3-\nu_2$, respectively. On that basis we determined from the fit a set of rotational, centrifugal distortion, and resonance interaction parameters (in general, 15 fitted parameters), which reproduce the 780 initial experimental energy levels of the (111) vibrational state with accuracies close to experimental uncertainties and better than sets of parameters known in the literature.

Acknowledgments

This research was supported by the Foundation of the President of the Russian Federation (Grant MK-4872.2014.2) and Deutsche Forschungsgemeinschaft (Grant BA 2176/3 – 2 and Grant BA 2176/4 – 1). Part of the work was made under the project FTI-120 of the Tomsk Polytechnic University. We thank B. Gerke for technical support.

Appendix A. Supplementary materials

Supplementary data associated with this paper can be found in the online version at http://dx.doi.org/10.1016/j.jqsrt.2014.03.027.

References

[1] Ulenikov ON, Onopenko GA, Gromova OV, Bekhtereva ES, Horneman VM. Re-analysis of the (100), (001), and (020) rotational structure of SO_2 on the basis of high resolution FTIR spectra. J Quant Spectrosc Radiat Transf 2013;130:220–32.

[2] Ulenikov ON, Bekhtereva ES, Horneman VM, Alanko S, Gromova OV. High resolution study of the $3\nu_1$ band of SO_2. J Mol Spectrosc 2009;255:111–21.

[3] Ulenikov ON, Bekhtereva ES, Horneman VM, Alanko S, Gromova OV, Leroy C. On the high resolution spectroscopy and intramolecular potential function of SO_2. J Mol Spectrosc 2009;257:137–56.

[4] Ulenikov ON, Bekhtereva ES, Gromova OV, Alanko S, Horneman VM, Leroy C. Analysis of highly excited "hot" bands in the SO_2 molecule: $\nu_2+3\nu_3-\nu_2$ and $2\nu_1+\nu_2+\nu_3-\nu_2$. Mol Phys 2010;108:1253–61.

[5] Ulenikov ON, Gromova OV, Bekhtereva ES, Bolotova IB, Leroy C, Horneman VM, et al. High resolution study of the $\nu_1+2\nu_2-\nu_2$ and $2\nu_2+\nu_3-\nu_2$ "hot" bands and ro-vibrational re-analysis of the $\nu_1+\nu_2/\nu_2+\nu_3/3\nu_2$ polyad of the $^{32}SO_2$ molecule. J Quant Spectrosc Radiat Transf 2011;112:486–512.

[6] Ulenikov ON, Gromova OV, Bekhtereva ES, Bolotova IB, Konov IA, Horneman VM, et al. High resolution analysis of the SO_2 spectrum in the 2600–2900 cm^{-1} region: $2\nu_3$, $\nu_2+2\nu_3-\nu_2$ and $2\nu_1+\nu_2$ bands. J Quant Spectrosc Radiat Transf 2012;113:500–17.

[7] Barbe A, Secroun C, Jouve P, Duterage B, Monnanteuil N, Bellet J, et al. High resolution spectra of $\nu_1+\nu_3$ and $\nu_1+\nu_2+\nu_3-\nu_2$ bands of SO_2. J Mol Spectrosc 1975;55:319–50.

[8] Pine AS, Dresselhaus G, Palm B, Davies RW, Clough SA. Analysis of the 4-μm $\nu_1+\nu_3$ combination band of SO_2. J Mol Spectrosc 1977;67:386–415.

[9] Lafferty WJ, Pine AS, Hilpert G, Sams RL, Flaud JM. The $\nu_1+\nu_3$ and $2\nu_1+\nu_3$ band systems of SO_2: line positions and intensities. J Mol Spectrosc 1996;176:280–6.

[10] Ahonen T, Alanko S, Horneman VM, Koivusaari M, Paso R, Tolonen AM, et al. A long path cell for the Fourier spectrometer BrukerIFS 120 HR: application to the weak $\nu_1+\nu_2$ and $3\nu_2$ bands of carbon disulfide. J Mol Spectrosc 1997;181:279–86.

[11] Maki AG, Wells JS. Wavenumber calibration tables from heterodyne frequency measurements(version 1.3). Gaithersburg, MD: National Institute of Standards and Technology; 1998.

[12] Horneman VM. Instrumental and calculation methods for Fourier transform infrared spectroscopy and accurate standard spectra [Thesis]. Acta Univ. Oul. A239; 1992. p. 127.

[13] Flaud JM, Perrin A, Salah LM, Lafferty WJ, Guelachvili G. A reanalysis of the (010), (020), (100), and (001) rotational levels. J Mol Spectrosc 1993;160:272–8.

[14] Flaud JM, Lafferty WJ. $^{32}S^{16}O_2$: a refined analysis of the $3\nu_3$ band and determination of equilibrium rotational constants. J Mol Spectrosc 1993;161:396–402.

[15] Lafferty WJ, Pine AS, Hilpert G, Sams RL, Flaud JM. The $\nu_1+\nu_3$ and $2\nu_1+\nu_3$ band systems of SO_2: line positions and intensities. J Mol Spectrosc 1996;176:280–6.

[16] Lafferty WJ, Flaud JM, Guelachvili G. Analysis of the $2\nu_1$ band system of SO_2. J Mol Spectrosc 1998;188:106–7.

[17] Watson JKG. Determination of centrifugal distortion coefficients of asymmetric-top molecules. J Chem Phys 1967;46:1935–49.

[18] Ulenikov ON, Tolchenov RN, Koivusaari M, Alanko S, Anttila R. High-resolution fourier transform spectra of CH_2D_2: pentade of the lowest interacting vibrational bands ν_4, ν_7, ν_9, ν_5, and ν_3. J Mol Spectrosc 1994;167:109–30.

[19] Müller HSP, Brunken S. Accurate rotational spectroscopy of sulfur dioxide, SO_2, in its ground vibrational and first excited bending states, $v_2=0, 1$, up to 2 THz. J Mol Spectrosc 2005;232:213–22.

[20] Ulenikov ON, Bekhtereva ES, Leroy C, Gromova OV, Fomchenko AL. On the determination of the intramolecular potential energy surface of polyatomic molecules: hydrogen sulfide and formaldehyde as an illustration. J Mol Spectrosc 2009;255:88–100.

[21] Nielsen HH. The vibration–rotation energies of molecules. Rev Mod Phys 1951;23:90.

[22] Papousek D, Aliev MR. Molecular vibrational–rotational spectra. Amsterdam, Oxford, New York: Elsevier Scientific Publishing Company; 1982.

[23] Liu AW, Ulenikov ON, Onopenko GA, Gromova OV, Bekhtereva ES, Wan L, et al. Global fit of the high resolution infrared spectrum of D_2S. J Mol Spectrosc 2006;238:23–40.

[24] Ulenikov ON, Liu AW, Bekhtereva ES, Onopenko GA, Gromova OV, Wan L, et al. Joint ro-vibrational analysis of the HDS high resolution infrared data. J Mol Spectrosc 2006;240:32–44.